Ultrafast terahertz photoconductivity in nanocrystalline mesoporous TiO_2 films

H. Němec,[1,a)] P. Kužel,[1] F. Kadlec,[1] D. Fattakhova-Rohlfing,[2] J. Szeifert,[2] T. Bein,[2] V. Kalousek,[3] and J. Rathouský[3]
[1]*Institute of Physics, v.v.i., Academy of Sciences of the Czech Republic, Na Slovance 2, 18221 Prague 8, Czech Republic*
[2]*Department of Chemistry and Biochemistry, University of Munich (LMU), Butenandtstrasse 5-13, 81377 Munich, Germany*
[3]*J. Heyrovský Institute of Physical Chemistry, v.v.i., Academy of Sciences of the Czech Republic, Dolejškova 3, 18223 Prague 8, Czech Republic*

(Received 8 October 2009; accepted 19 January 2010; published online 8 February 2010)

Terahertz time-resolved spectroscopy is used to investigate the transport of photoexcited electrons in nanocrystalline mesoporous TiO_2 films prepared by the recently proposed "brick and mortar" technology [Szeifert *et al.*Chem. Mater. **21**, 1260 (2009)] with a variable fraction of nanocrystalline titania "bricks" and amorphous titania "mortar." Both long- and short-range conductivity is significantly enhanced upon calcination. After an ultrafast (subpicosecond) regime where the intrananograin conductivity dominates, the electron conductivity becomes limited by the interaction of electrons with the amorphous mortar. Comparison of the experimental results with Monte Carlo simulations of the electron motion allows us to determine the crystalline grain size after calcination and the yield of mobile photocarriers. © *2010 American Institute of Physics*.
[doi:10.1063/1.3313936]

Dye-sensitized nanostructured semiconductors are promising materials for photovoltaic applications as they offer high power conversion efficiency and their fabrication may capitalize on low-cost thin-film technologies.[1] The progress in past years in the functional design of the Grätzel cells makes nanostructured TiO_2 films particularly interesting from the point of view of the fundamental science and applications.[2,3] Both nanoscopic and long-range charge transport properties strongly depend on the morphology of these complex systems.

Recently, a so-called "brick and mortar" process based on the fusion of preformed TiO_2 nanocrystals (bricks) with a surfactant-templated amorphous TiO_2 matrix (mortar) has been proposed for the preparation of nanostructured TiO_2 films with highly crystalline and porous structures after calcination at low temperatures.[4] Identical chemical composition of the bricks and mortar leads to efficient seeded growth of the crystalline phase upon calcination. The physicochemical properties of the final structures are controlled by the fraction of the bricks.

In this letter, we study the ultrafast photoconductivity spectra of such films by means of optical pump—terahertz probe experiments. This contact-free technique probes the transport of photoexcited charges on subpicosecond (sub-ps) to nanosecond time scales[5] and the measured transient spectra directly reflect the charge motion on the scale of the size of nanostructural components.

The details of the sample preparation are given in Ref. 4. Briefly, TiO_2 nanoparticles were prepared by reaction of $TiCl_4$ in benzyl alcohol at 60 °C for 20 h. The particles were separated by centrifugation and redispersed in solution of polyethylene oxide block copolymer Pluronic P123 (BASF) in tetrahydrofurane with formation of transparent colloidal solution. Subsequently, the desired amount of sol-gel solution prepared by hydrolysis of tetraethyl orthotitanate with concentrated hydrochloric acid was added followed by stirring for several minutes. The films were deposited by dip-coating at 23 °C and a relative humidity of 45% at a withdrawal rate of 1.8 mm/s.

The fraction of the crystalline phase (bricks) was 0%, 10%, and 70% for the samples A, B, and C, respectively. One set of samples was investigated as-grown (samples A1, B1, and C1), the other set was calcined at 300 °C for 30 min (samples A2, B2, and C2). The transient terahertz spectra were measured in a custom made setup[6] powered by an amplified Ti:sapphire laser system. The samples were excited by femtosecond pulses at 270 nm typically with 5×10^{14} photons/cm^2 per pulse. The experiments were performed in a rough-vacuum chamber with a noncollinear arrangement of the pump and probe beams yielding a time resolution of ~1 ps.[6]

We first measured the variation of the maximum of transmitted transient terahertz pulse with the pump-probe delay τ_p. This signal is proportional to the population of mobile electrons and to their mean terahertz mobility.[6] The observed kinetics is composed of a sub-ps or ps decay and of a slower component which does not decay completely within ~200 ps (Fig. 1). The noncalcined sample without the crystalline phase (A1) does not yield a detectable signal, and for the sample B1 (small crystallinity, noncalcined), only the sub-ps decay component exceeded the noise level. This means that the quantum yield of mobile carriers in noncalcined samples is small since a significant part of incident photons may excite amorphous or organic parts of the sample. The relative contribution of the short-lived component is higher for less crystalline and noncalcined samples. It is then probably (similarly as in Ref. 6) related to carriers

a)Electronic mail: nemec@fzu.cz.

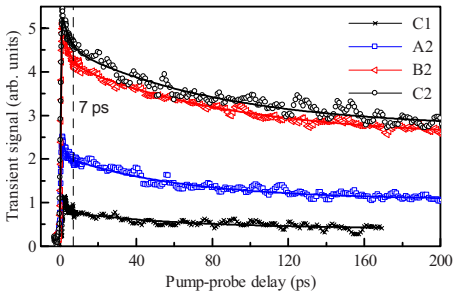

FIG. 1. (Color online) Time evolution of mean transient terahertz conductivity. Symbols: experimental data; lines: fit by a biexponential function with a background.

initially excited in crystalline nanograins which diffuse to grain boundaries where they are trapped.

In order to elucidate the character of the transport within the slow component we measured transient terahertz spectra at several delays after photoexcitation. We found that the shape of the spectra does not vary for delays between 7 and 200 ps which means that the conductivity mechanism does not change during this time and that the signal decay stems from the decrease of the mobile carrier concentration. As shown in Ref. 6, the transient effective conductivity $\Delta\sigma_{\mathrm{eff}}(f,\tau_{\mathrm{p}})$ is proportional to the spectrum of the measured transient terahertz pulse $\Delta E(f,\tau_{\mathrm{p}})$. Owing to the local (depolarization) fields the measured response $\Delta\sigma_{\mathrm{eff}}(f,\tau_{\mathrm{p}})$ differs from the microscopic conductivity $\Delta\sigma(f,\tau_{\mathrm{p}})$ of the charges within nanoparticles. For the percolated network of high-permittivity nanoparticles with 35% of air voids, the microscopic conductivity is $\Delta\sigma=\Delta\sigma_{\mathrm{eff}}/0.55$.[7] In Fig. 2 we plot the microscopic conductivity $\Delta\sigma$ per unit charge normalized by the number of photons absorbed in a unit volume. It equals the product of quantum yield of mobile carriers $\xi(\tau_{\mathrm{p}})$ at the given pump-probe delay and of their complex mobility spectrum $\mu(f)$. The character of the spectrum is typical for carriers exhibiting localization on nanometer scale as follows:[7] Re μ increases with frequency and Im μ is negative in the terahertz range. In addition, namely, in the most crystalline samples C2 and B2, we observe a clear fingerprint of the long-range transport given by the nonvanishing extrapolation of Re μ to zero frequency (called low-frequency mobility below). This is a signature of the percolation of photoconducting parts of the nanocomposite.

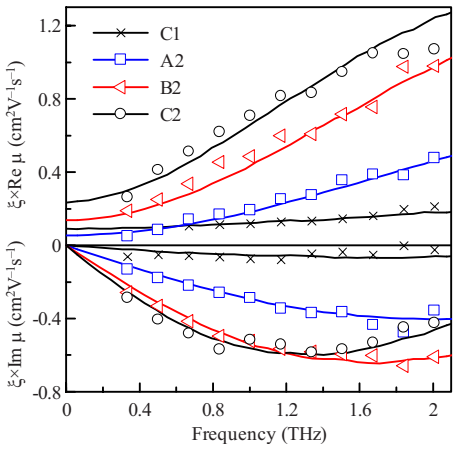

FIG. 2. (Color online) Transient terahertz conductivity spectra measured 7 ps after photoexcitation. Symbols: experimental data; lines: simulation.

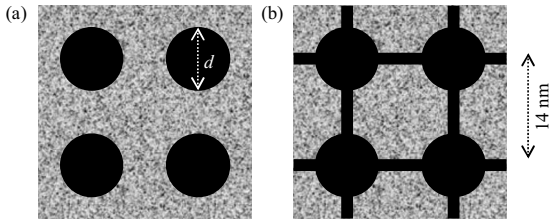

FIG. 3. Schemes of the structures used for the calculation of electron mobility spectrum. (a) Isolated crystalline TiO_2 nanospheres (black) are embedded in an amorphous tissue (gray) exhibiting a certain low photoconductivity. (b) Crystalline TiO_2 nanospheres are linked by narrow connectors of crystalline TiO_2 (black) and the amorphous tissue (gray) does not exhibit any photoconductivity.

We carried out a series of Monte Carlo simulations of the carrier motion within nanostructured samples in order to calculate their spectral response $\mu(f)$. Such simulations provide the mobility of carriers, and by comparison with the experimental data we are able to estimate the yield ξ of mobile carriers. The calculations were performed similarly as in Ref. 7 by using the Kubo formula to relate the carrier mobility spectrum to the autocorrelation function of the velocity of their thermal motion.

Our films comprise three following components: the nanocrystals (we assume they have the same properties as bulk single crystals, e.g., the carrier momentum scattering time $\tau_{\mathrm{D}}=100$ fs), the amorphous phase (which possibly may show some measurable photoconductivity in the terahertz range) and voids (with no conductivity). The spatial distribution of these phases depends on the "brick" fraction and on the calcination conditions of the films.[4] The exact distribution of these phases is unknown, therefore we considered two limit cases. First, we calculated the response of periodic lattice of isolated nanospheres of crystalline TiO_2 surrounded by a less conductive medium characterized by a shorter momentum scattering time [Fig. 3(a)]. In the second case, the nanospheres of crystalline TiO_2 are connected by narrow crystalline channels and the entire structure is surrounded by a nonconducting medium [Fig. 3(b)]. The periodicity of the lattice was 14 nm to reflect the periodicity of the polymer template.[4] We did not consider any air voids since they are taken into account by the above mentioned effective medium approximation and since they cannot influence the degree of the electron localization in the nanospheres which essentially determines the mobility spectrum.

Both series of simulations yield nearly identical mobility spectra $\mu(f)$ which are in a very good agreement with the measured ones (Fig. 2). The shape of the spectra is due to the localization of electrons in the nanospheres; the probability $p_{\mathrm{C}\to\mathrm{A}}$ that the electron passes from the crystalline nanosphere to the amorphous surroundings upon its interaction with the nanosphere boundary is $\lesssim 10\%$. The proportion between the real and imaginary parts of the spectrum is controlled by the diameter of nanospheres. This allows us to determine with a good precision the mean size of the grains of calcined samples (Table I). The low-frequency mobility which is related to the long-range transport can originate from several distinct processes. In the first series of simulations, it stems essentially from electrons generated in the amorphous tissue. In the second series of simulations, it is due to the photoconducting connectors. An additional contribution comes also from a small nonzero probability $p_{\mathrm{C}\to\mathrm{A}}$.

TABLE I. Summary of the properties of the samples studied; d is the mean diameter of crystalline nanograins: for noncalcined samples the nominal size of crystalline particles used for the sample preparation is indicated. The values of d for calcined samples and those of the yield ξ were obtained from fits of the experimental data.

Sample	Brick fraction (%)	Calcination (°C)	d (nm)	ξ at 7 ps (%)
A1	0	⋯	⋯	⋯
B1	10	⋯	≈4–5 (Ref. 4)	<0.2
C1	70	⋯	≈4–5 (Ref. 4)	3.6
A2	0	300	3.9	18
B2	10	300	4.7	25
C2	70	300	5.8	20

These findings along with the structural data from Fig. 4 and from Ref. 4 allow understanding the electron transport mechanisms in the films. The noncalcined sample A1 did not exhibit a measurable signal, i.e., the electron mobility in the noncalcined "mortar" is immeasurably low. The B1 sample containing 10% of "bricks" exhibited a very low sub-ps photoconductivity which corresponds to the low fraction of the bricks. The short lifetime indicates the presence of a large density of traps in this sample. The noncalcined sample C1 is composed of 70% "bricks" of 4–5 nm in size[4] surrounded by the "mortar," i.e., the model from Fig. 3(a) is appropriate for this sample. The small nonvanishing low-frequency mobility indicates that $p_{C\to A}$ is nonzero (electrons can pass to the amorphous phase). The low quantum yield of mobile electrons at 7 ps (3.6%, Table I) may be related to the absorption of photons in the nonconducting phase or in the organic vehicle. The quantum yield at this longer time is also limited by electron trapping as can be inferred from the presence of a strong short-lived component in Fig. 1.

The calcination leads to a seeded growth of the crystalline phase, as indicated, e.g., by the enhancement of the (101) reflection in the x-ray diffraction patterns (Fig. 4). In the terahertz spectra this is best observed in the sample A2 in which the amorphous phase was partially transformed into quite large (~3.9 nm) crystallites (Table I). The long-lived component of the photoconductivity is substantially enhanced which shows that the density of electron traps was significantly reduced. In the B2 and C2 samples, the calcination leads to a partial crystallization of the "mortar" and also to the enlargement of the "bricks." This manifests itself as the increase in the mean diameter of nanospheres determined from the measured mobility spectra (Table I). The low-frequency mobility markedly increases with increasing fraction of the crystalline "bricks" which means that the electrical connectivity of individual nanoparticles becomes enhanced, in agreement with the scanning electron microscope images from Ref. 4. It is not probable, though, that very narrow crystalline connectors form, as depicted in Fig. 3(b). It is reasonable to assume that the electron mobility in the "mortar" improves upon calcination and relatively wide areas of such a "mortar" then lead to the observed enhancement of the low-frequency mobility. Note finally that the yield of mobile carriers increases nearly by an order of magnitude upon calcination; however, it still reaches about 20% only. This should be related to the fact that a part of the incident photons generates electrons in the amorphous phase and that a certain fraction of electrons may be captured in traps within 7 ps after photoexcitation.

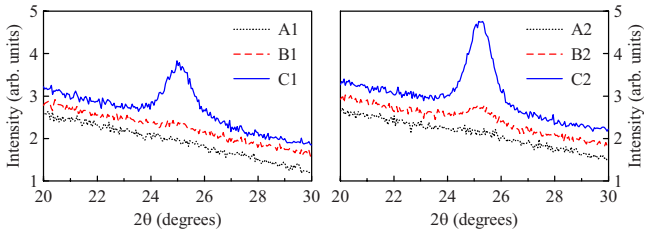

FIG. 4. (Color online) Comparison of the (101) anatase reflection in x-ray diffraction patterns from the as-grown (left panel) and calcined samples (right panel).

To summarize, electron transport in the terahertz regime was studied in nanostructured TiO_2 films prepared by the "brick and mortar" technology. The photoexcited electron mobility in noncalcined films is very low due to the low crystallinity of the films and a high density of traps. Upon calcination the crystallinity significantly improves and the density of traps is substantially reduced. The connectivity of the crystallites becomes better with increasing fraction of intrinsic "bricks," nevertheless the structure is not fully percolated and the electrons are still strongly localized in the crystallites.

The work was supported by the Czech Science Foundation (Grant Nos. 202/09/P099, 104/08/0435-1, and 203/08/H032) and by the Academy of Sciences of the Czech Republic (Projects A100100902, AVOZ10100520), and by the German Science Foundation (NIM Cluster at the University of Munich).

[1]M. Grätzel, Nature (London) **414**, 338 (2001).
[2]M. Grätzel, J. Photochem. Photobiol., A **164**, 3 (2004).
[3]Q. Wang, S. Ito, M. Grätzel, F. Fabregat-Santiago, I. Mora-Seró, J. Bisquert, T. Bessho, and H. Imai, J. Phys. Chem. B **110**, 25210 (2006).
[4]J. M. Szeifert, D. Fattakhova-Rohlfing, D. Georgiadou, V. Kalousek, J. Rathouský, D. Kuang, S. Wenger, S. M. Zakeeruddin, M. Grätzel, and T. Bein, Chem. Mater. **21**, 1260 (2009).
[5]F. A. Hegmann, O. Ostroverkhova, and D. G. Cooke, *Photophysics of Molecular Materials* (Wiley, New York, 2006), Chap. 7, pp. 367–428.
[6]L. Fekete, P. Kužel, H. Němec, F. Kadlec, A. Dejneka, J. Stuchlík, and A. Fejfar, Phys. Rev. B **79**, 115306 (2009).
[7]H. Němec, P. Kužel, and V. Sundström, Phys. Rev. B **79**, 115309 (2009).